Jestr

Journal of Engineering Science and Technology Review 13 (5) (2020) 169 - 175

JOURNAL OF
Engineering Science and Technology Review

Research Article

www.jestr.org

Adaptive Multiscale Block Compressed Sensing of Images based on Gray Level Co-Occurrence Matrix

Jinfeng Li, Jinnan Guo, Shun Cao* and Yutong Zhao

College of Information Engineering, Shenyang University of Chemical Technology, Shenyang 110142, China

Received 19 July 2020; Accepted 11 September 2020

Abstract

In conventional block compressed sensing (BCS), the images are divided into small fixed-size blocks sampled at the same sub-rate. The sparsities and high-frequency components of the images are ignored, and the reconstruction qualities of the complex texture images are poor. An adaptive multiscale variant of the block compressed sensing was proposed to reconstruct the texture details of the images. The texture features of the images were obtained from the high-frequency components by the three-level wavelet transform and analyzed on the basis of the gray level co-occurrence matrix. A mathematical model was established to adjust the block sizes of the images automatically and allocate the limited sampling resource adaptively. The smoothed projected Landweber (SPL) was utilized to reconstruct the images. The accuracy of the proposed algorithm was verified by the simulation experiments. Results demonstrate that the texture details of the reconstructed images are abundant. The image edges are also clear, and the blocking artifacts are effectively eliminated. The reconstruction qualities of images, especially the partial images, are considerably improved at different sub-sampling rates. The proposed algorithm achieves a 2.42–3.3 dB gain in reconstruction PSNR for the Barbara image over the original BCS-SPL at a sub-sampling rate of 0.3. No remarkable differences are noted between the reconstructed and original texture blocks in visual sensation. The proposed algorithm provides evidence for the compression and reconstruction of the images with complex texture details.

Keywords: Block compressed sensing, Adaptive sampling, Multiscale block, Texture, Gray level co-occurrence matrix

1. Introduction

Compressed sensing (CS) [1-2] overcomes the limitation that the sampling frequency must be at least twice as fast as the signal bandwidth. The sampling and compression processes are integrated, which considerably decreases the sampling cost. The original signal is first transformed into the sparse array and then projected onto a low-dimensional space by the measurement matrix at the transmitting end. The less measured data can be reconstructed using the convex optimization method at the receiving end. CS has become an important reform in the field of information in recent years, thus attracting considerable attention and demonstrating its wide application in image processing, wireless sensor networks, communications, optical/remote sensing imaging, and applied mathematics [3-5].

However, the order of the measurement matrix correspondingly increases with the image pixels when compressed sensing is applied to two-dimensional images. The storage and calculation of the matrix face massive challenges. The storage requirements are high, the reconstruction time is long, and the reconstruction qualities are poor. The images in block compressed sensing (BCS) [6-7] are divided into fixed-size blocks. Each block is independently sampled by the same measurement matrix and reconstructed. The size of the measurement matrix is decreased, the reconstruction time is shortened, and the sampling efficiency is improved. Nevertheless, the sparsities of the images are not fully utilized, and the allocation of sampling resources is unreasonable due to the fixed block size and same sub-sampling rate for each block. The blocking artifacts are introduced during the reconstruction process, and the rough block edges are produced in the reconstructed images with complex textures.

Scholars have conducted extensive studies on image partition and blocking artifact elimination to improve reconstruction qualities of the images [8-14]. However, the high-frequency components of the images are ignored in the reconstruction process, and the reconstruction qualities of texture details are poor. Therefore, accurate measurement of the texture complexity, multiscale block division, and adaptive allocation of sub-sampling rates are urgent problems that must be solved.

This study obtains the high-frequency components of the images and analyzes the texture complexity. A mathematical model is established to partition the images into variable-size blocks automatically and allocate the sub-sampling rates adaptively. Moreover, the images are reconstructed. The blocking artifacts are effectively eliminated, and the reconstruction qualities of the images, especially the texture details of blocks, are improved. Thus, a reference for developing and optimizing the adaptive multiscale block BCS of images is provided.

2. State of the Art

At present, scholars have performed numerous studies on BCS. The sparsity is crucial in CS reconstruction. The reconstruction qualities of images can be improved by fully utilizing the sparsity of the images. The BCS-SPL algorithm

*E-mail address: ffagcao95@163.com
ISSN: 1791-2377
doi:10.25103/jestr.135.22

was suggested by Mun S. [7] to enforce sparsity via dual-tree complex wavelet transform and bivariate shrinkage. The smoothed projected Landweber (SPL) and Wiener filtering were applied to reconstruct the images rapidly and eliminate the blocking artifacts. However, the distributed sub-sampling rates to image blocks were unreasonable, and the reconstruction qualities were poor. Spurthi S. [8] employed the discrete cosine transform, discrete wavelet transform, and contourlets as the sparsity transform. However, the influence of texture distribution on the reconstruction quality was not considered. Haltmeier M. [9] improved the sparsity transform. Unde A. S. [10] adjusted the sparsities of the original images based on l_1-norm minimization to increase the sampling efficiency. However, the reconstruction qualities of texture details were poor. Cao Y. [11] adopted the optimized sequence and weighted sampling to adjust the sparsities of image blocks and improve the reconstruction qualities. Nevertheless, the texture complexity was disregarded. Eslahi N. [12] enforced local and non-local 3-dimensional sparsity to obtain the local smoothing and non-local self-similarity information. However, the high-frequency components of the images were not considered. Bigot J. [13] and George S. N. [14] designed a random measurement matrix, but the texture complexity of the images was not calculated. The variable sub-sampling rates should be set in accordance with the texture complexity of the image blocks. The MS-BCS-SPL algorithm was presented by Fowler J. E. [15] to decompose the images by a three-level wavelet transform. The different sub-sampling rates were set to different levels of the wavelet decomposition. However, the same sub-sampling rate for each level of blocks caused an unreasonable allocation of sampling resource. The rough block edges are found in the reconstructed images with complex textures. The ED-MS-BCS-SPL algorithm was suggested by Li Y. [16] to allocate the total sub-sampling rates to each block of the levels following the edge structures and direction characteristics of the images adaptively. The reconstruction performance was improved. Nevertheless, only the edge structures of low-frequency components were measured. The image blocks were classified into texture and plain blocks [17-18]. The blocking artifacts were eliminated by adaptive weighted filtering based on two-dimensional neighborhood features. The reconstruction qualities of the edge details were improved. However, the detection time of the plain blocks was long. The adaptive sampling can be employed to adjust the sub-sampling rate of each block based on the texture feature. Accurately measuring the texture complexity of the image blocks is important. Li R. [19] utilized spatial entropy to measure the texture features of image blocks. However, this method is unsuitable for images with complex textures. Wang Y. [20] promoted the reconstruction quality by adaptively assigning the sub-sampling rates due to the gray entropy of the image blocks. Nevertheless, the correlation between image elements was not considered. Cai X. [21] measured the texture structures by the total variation difference method, but the accuracy of the method was poor.

The simulation experiments were performed to improve the sparsities of the original images. Few studies have explored the adaptive sub-sampling rate and texture complexity measurement to reconstruct the texture details of the images. The texture information of the images was obtained in the present study through a three-level wavelet transform. The entropy of the gray-level co-occurrence matrix was utilized to calculate the texture complexity of the image blocks accurately. Furthermore, a mathematical model was established to determine the block size and allocate the sub-sampling rates to each block adaptively according to the image textures. The natural images were compressed and reconstructed, and the blocking artifacts were effectively eliminated, thereby providing a basis for the optimization of the adaptive multiscale BCS of images.

The remainder of this study is organized as follows. Section 3 describes the measurement method of texture complexity and establishes the calculation model to achieve multiscale blocks and adaptive sub-sampling rates. Section 4 reconstructs the natural images with different texture complexities and analyzes the reconstruction quality. Finally, Section 5 summarizes the conclusions.

3. Methodology

3.1 CS theory

CS theory is based on the concept of signal sparsity. Let $x \in R^{N\times 1}$ be the real-valued N-dimensional signal. Suppose that the coefficients are sparse or compressible under a set of orthogonal bases $\psi = [\psi_1, \psi_2, \cdots \psi_N] \in R^{N\times N}$. The signal can then be sub-sampled by the measurement matrix ϕ, and the obtained vector is as follows:

$$y = \phi x = \phi\psi\theta \tag{1}$$

where ϕ is an $M \times N (M \le N)$ measurement matrix, x is an $N \times 1$ original input signal, and y is the $M \times 1$ measurement vector. The signal x can be accurately recovered from y assuming that the measurement matrix ϕ satisfies restricted isometry property and θ is sparse. When CS is applied to two-dimensional images, the scale of the measurement matrix is substantially large, which is up to the magnitude of 10^4–10^6. The storage requirements are relatively high, and the related calculation cost is huge.

3.2 BCS theory

In the sampling process of BCS, the original image (N pixels) is partitioned into b non-overlapping blocks with a size of $B \times B$. The block is arranged in a column, which is denoted as x_i, and independently sampled by the same measurement matrix. The obtained vector sets are as follows:

$$y = \{y_i | y_i = \phi_a x_i, i = 1,2,\cdots b\} \tag{2}$$

where ϕ_a is an $m \times B^2$ measurement matrix, $m = \lfloor sr \times B^2 \rfloor$ is the number of samples, $sr = M / N$ (M samples from N pixels) is the sub-sampling rate, and x_i is the ith block of the original image.

Each block in BCS is independently sampled and reconstructed. The storage and calculation are performed on the measurement matrix ϕ_a. The scale of the measurement matrix no longer increases with the size of the original image. Moreover, each block adopts the same measurement matrix. Only the matrix ϕ_a is stored at the receiving end. The storage resource is saved, the calculation cost is reduced, and real-time performance is improved. However, the differences in textures are present among the blocks, and the sparsities are uneven. The reconstruction effects of the blocks are different. False boundaries and fuzzy shadows

between adjacent blocks appear when the blocks with different reconstruction effects are reconstructed into an image. The brightness of each block is different, demonstrating a blocking artifact.

3.3 Proposed adaptive multiscale BCS

The reconstruction effect is closely related to the texture complexity of the image. Limited sample data can obtain good reconstruction qualities for the plain blocks, while additional sample data are required for the complex texture blocks. The image is divided into fixed-size blocks in most of the literature, which is convenient for operation. However, the reconstruction qualities of the complex texture blocks are poor, thereby decreasing the effect of the entire image. The block sizes and sub-sampling rates should be adaptively adjusted in accordance with the texture features of the image blocks. The large block sizes and low sub-sampling rates are set to increase the compression ratios of the plain blocks, while the small block sizes and high sub-sampling rates are set to increase the reconstruction qualities of texture blocks. The texture feature of each block is fully utilized to allocate the limited sampling resource effectively, thereby improving the reconstruction quality of the entire image. The original image is decomposed by wavelet transform to generate low- and high-frequency components. The low-frequency component concentrates on the energy of the original image, while the high-frequency component represents the texture information of the image. The algorithm for BCS is improved in the present study, and the high-frequency component of the image is employed in the reconstruction process. The block sizes and sub-sampling rates are adjusted on the basis of the texture complexity of the image blocks. The PSNR of the proposed algorithm is also increased.

The entropy of the gray level co-occurrence matrix is utilized to measure the texture complexity of the image. The texture feature of an image is determined by the number of pixels with different complexities. Therefore, two pixels with the same complexity must be available, that is, a certain spatial relationship exists between the pixels. The spatial relationship is statistically analyzed, and a matrix representing the texture information is obtained, which is a gray-level co-occurrence matrix. The gray-level co-occurrence matrix is described as the probability that a pixel with gray level *i* reaches another pixel with gray level *j* along a predetermined path *d*, that is, $P_d(i,j)(i,j=0,1,2,\cdots L-1)$: where *L* is the gray level, and *d* indicates the distance and direction between the two pixels. The commonly adopted direction angles are 0°, 45°, 90°, and 135°. The gray level of the original image is quantized to 0–15 to decrease the computational burden. The gray-level co-occurrence matrix is expressed as follows:

$$P_d=\begin{bmatrix} P_d(0,0) & P_d(0,1) & \cdots & P_d(0,L-1) \\ P_d(1,0) & P_d(1,1) & \cdots & P_d(1,L-1) \\ \cdots & \cdots & \cdots & \cdots \\ P_d(i,0) & P_d(i,1) & \cdots & P_d(i,L-1) \\ \cdots & \cdots & \cdots & \cdots \\ P_d(L-1,0) & P_d(L-1,1) & \cdots & P_d(L-1,L-1) \end{bmatrix} \quad (3)$$

The entropy of the gray-level co-occurrence matrix is:

$$H=-\sum_{i=0}^{L-1}\sum_{j=0}^{L-1}P_d(i,j)\log P_d(i,j) \quad (4)$$

The texture complexity of the image block is:

$$T_c=\frac{1}{B\times B}H \quad (5)$$

The multiscale block and adaptive sub-sampling rate are realized on the basis of the texture complexity of the images. The blocks with complex textures are subdivided and allocated with high sub-sampling rates, while those with plain textures are allocated with low sub-sampling rates. The detailed steps are presented as follows.

Step 1) The image is decomposed by a three-level wavelet transform. The low-frequency coefficients are set to zero, and the high-frequency components are subjected to wavelet inverse transform to obtain the image *T*.

Step 2) The image *T* is divided into blocks with a size of $B\times B$, where *B* is 32. The texture complexity T_c of each image block is calculated in accordance with formula (5). The threshold T_1 of the texture complexity is set. If T_c is less than T_1, then the sub-sampling rate is adaptively allocated:

$$sr_{1\_i}=(S_1-S_{\min})\times h_1\times H_{1\_i}/\sum_{i=1}^{h_1}H_{1\_i}+S_{\min},T_c\le T_1 \quad (6)$$

where h_1 is the number of image blocks with the size of $B\times B$, and $S_{\min}$ is [17]:

$$S_{\min}=\begin{cases} sr/2 & 0<sr\le 0.1 \\ 0.05 & 0.1<sr\le 1 \end{cases} \quad (7)$$

If T_c is more than T_1, then the block is divided into four sub-blocks with a size of $B/2\times B/2$.

Step 3) The texture complexity T_c of each image sub-block with the size of $B/2\times B/2$ is calculated in accordance with formula (5). The threshold T_2 of the texture complexity is set. If T_c is less than T_2, then the sub-sampling rate is adaptively allocated:

$$sr_{2\_i}=(S_2-S_{\min})\times h_2\times H_{2\_i}/\sum_{i=1}^{h_2}H_{2\_i}+S_{\min},T_c\le T_2 \quad (8)$$

If T_c is more than T_2, then the block is divided into four sub-blocks with a size of $B/4\times B/4$.

Step 4) The texture complexity T_c of each image sub-block with the size of $B/4\times B/4$ is calculated in accordance with formula (5). The threshold T_3 of the texture complexity is set. If T_c is less than T_3, then the sub-sampling rate is adaptively allocated:

$$sr_{3\_i}=(S_3-S_{\min})\times h_3\times H_{3\_i}/\sum_{i=1}^{h_3}H_{3\_i}+S_{\min},T_c\le T_3 \quad (9)$$

If T_c is more than T_3, then the block is divided into four sub-blocks with a size of $B/8\times B/8$. The sub-sampling rate is adaptively allocated:

$$sr_{4\_i} = (S_4 - S_{\min}) \times h_4 \times H_{4\_i} / \sum_{i=1}^{h_4} H_{4\_i} + S_{\min} \tag{10}$$

where

$$S_1 = \sum_{i=1}^{h_1} H_{1\_i} / S_{um}\_H \times sr / h_1 /(B \times B) + S_{\min}$$

$$S_2 = \sum_{i=1}^{h_2} H_{2\_i} / S_{um}\_H \times sr / h_2 /(B/2 \times B/2) + S_{\min}$$

$$S_3 = \sum_{i=1}^{h_3} H_{3\_i} / S_{um}\_H \times sr / h_3 /(B/4 \times B/4) + S_{\min} \tag{11}$$

$$S_4 = \sum_{i=1}^{h_4} H_{4\_i} / S_{um}\_H \times sr / h_4 /(B/8 \times B/8) + S_{\min}$$

$$S_{um}\_H = \sum_{i=1}^{h_1} H_{1\_i} + \sum_{i=1}^{h_2} H_{2\_i} + \sum_{i=1}^{h_3} H_{3\_i} + \sum_{i=1}^{h_4} H_{4\_i}$$

The sampling number of the sub-block is calculated following the corresponding sub-sampling rate, and the measurement matrix is determined. All the sub-blocks are synchronously sampled, and the measurement vector sets are obtained.

Step 5) The high-frequency components of the image are reconstructed by the SPL [7], which is normalized and combined with the low-frequency pre-reconstructed image to obtain a high-quality reconstructed image.

The flow diagram of the proposed algorithm is shown in Fig. 1.

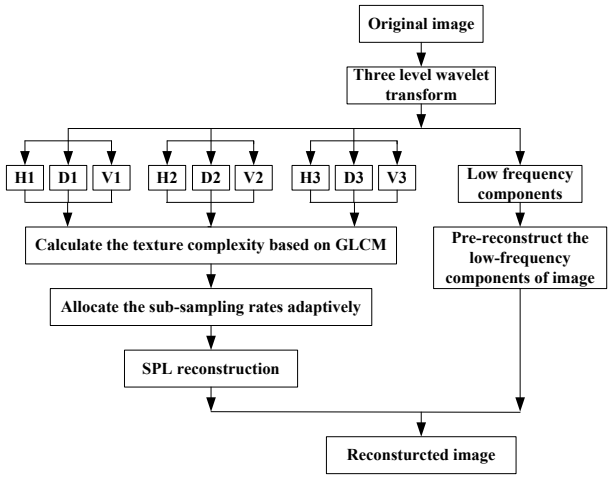

Fig. 1. Flow diagram of the proposed algorithm

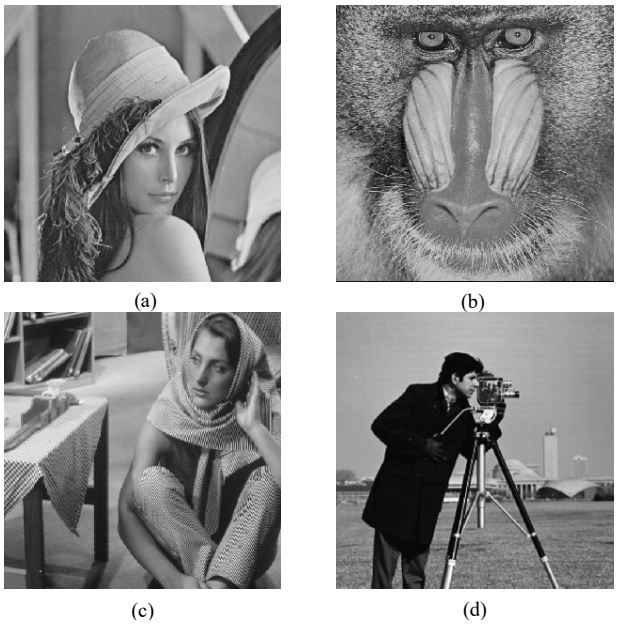

Fig. 2. Test gray images (a)Lenna (b)Mandrill (c)Barbara (d)Cameraman

4. Result analysis and discussion

The gray images with different texture complexities are reconstructed, and the reconstruction qualities are analyzed in accordance with the proposed method in Section 3.3. The test gray images are Lena, Mandrill, Barbara, and Cameraman. The size is 512 × 512 pixels as shown in Fig. 2. The discrete cosine transform (DCT) is adopted as the measurement matrix. The test images are decomposed by a three-level 9/7 orthogonal wavelet transform. The high-frequency components of the images are pre-reconstructed and divided into non-overlapping image blocks. The texture complexity of the image blocks is measured by the gray level co-occurrence matrix to determine the block sizes and allocate the sub-sampling rates adaptively. The image blocks with complex textures are small and sampled at high sub-sampling rates, while those with plain textures are large and sampled at low sub-sampling rates. The sparsities of the images are considered, and the limit sampling resource is effectively utilized. The images are reconstructed by the SPL method. The reconstruction quality of the proposed algorithm is compared with BCS-SPL-DCT, BCS-SPL-DWT, and BCS-SPL-DDWT [7].

4.1 Parameter settings

The variable block sizes are 32, 16, 8, and 4. The threshold of texture complexity is determined in accordance with the simulation experiments and set at the average value of texture complexity in this study. The gray levels of the images are quantized to 0–15 to reduce the calculation cost. The distance d is 1, and the angle is 0°.

4.2 Performance comparison of different reconstruction algorithms

The PSNR at the sub-sampling rates (M/N) of 0.2, 0.3, 0.4, and 0.5 is listed in Table 1. The table reveals that the reconstruction quality of the proposed algorithm is improved. The advantage is particularly evident with the increase in the sub-sampling rate. The PSNR of the proposed algorithm at the sub-sampling rates of 0.2–0.5 is 0.6–5.34, 0.5–5.57, and 0.07–4.77 dB higher than BCS-SPL-DCT, BCS-SPL-DWT, and BCS -SPL-DDWT, respectively. The comparison results with the three other test images reveal that the reconstruction PSNR for Barbara image is substantially increased. At the sub-sampling rate of 0.3, the PSNR of the proposed algorithm is 2.42, 3.3, and 2.71 dB higher than BCS-SPL-DCT, BCS-SPL-DWT, and BCS-

SPL-DDWT, respectively. The global views and local details of the reconstructed images at the sub-sampling rate of 0.3 are shown in Figures 3–5. The images reveal that the blocking artifacts are effectively eliminated, the texture details of reconstructed images are abundant, and the image edges are clear. Good visual qualities are also yielded. The reconstruction effect of blocks with complex textures, such as the hair in the Mandrill image, the scarf in the Barbara image, and the camera in the Cameraman image, is considerably improved. This phenomenon is due to the allocation of high sub-sampling rates to the complex texture blocks with small block sizes. The sampling resource is efficiently utilized, and the texture details of the images are fully reconstructed. At the sub-sampling rate of 0.3, no remarkable differences are noted between the reconstructed and original texture blocks in visual sensation.

Table 1. Reconstruction PSNR in dB

Image	Algorithm	Sub-sampling rate(M/N)			
		0.2	0.3	0.4	0.5
Lena	BCS-SPL-DCT	30.45	32.47	34.23	35.78
	BCS-SPL-DWT	30.79	32.89	34.70	36.28
	BCS-SPL-DDWT	31.29	33.40	35.16	36.74
	Proposed	**32.38**	**35.22**	**37.43**	**38.72**
Mandrill	BCS-SPL-DCT	21.32	22.32	23.35	23.67
	BCS-SPL-DWT	21.62	22.64	23.65	24.74
	BCS-SPL-DDWT	21.85	22.89	23.95	25.09
	Proposed	**21.92**	**23.57**	**25.19**	**27.11**
Barbara	BCS-SPL-DCT	24.42	25.98	27.38	29.01
	BCS-SPL-DWT	23.77	25.10	26.51	28.02
	BCS-SPL-DDWT	24.15	25.69	27.23	28.82
	Proposed	**25.54**	**28.40**	**30.88**	**33.59**
Cameraman	BCS-SPL-DCT	29.97	32.95	35.68	37.84
	BCS-SPL-DWT	29.74	32.94	35.57	37.91
	BCS-SPL-DDWT	30.34	33.71	36.44	38.93
	Proposed	**32.84**	**34.71**	**39.02**	**43.18**

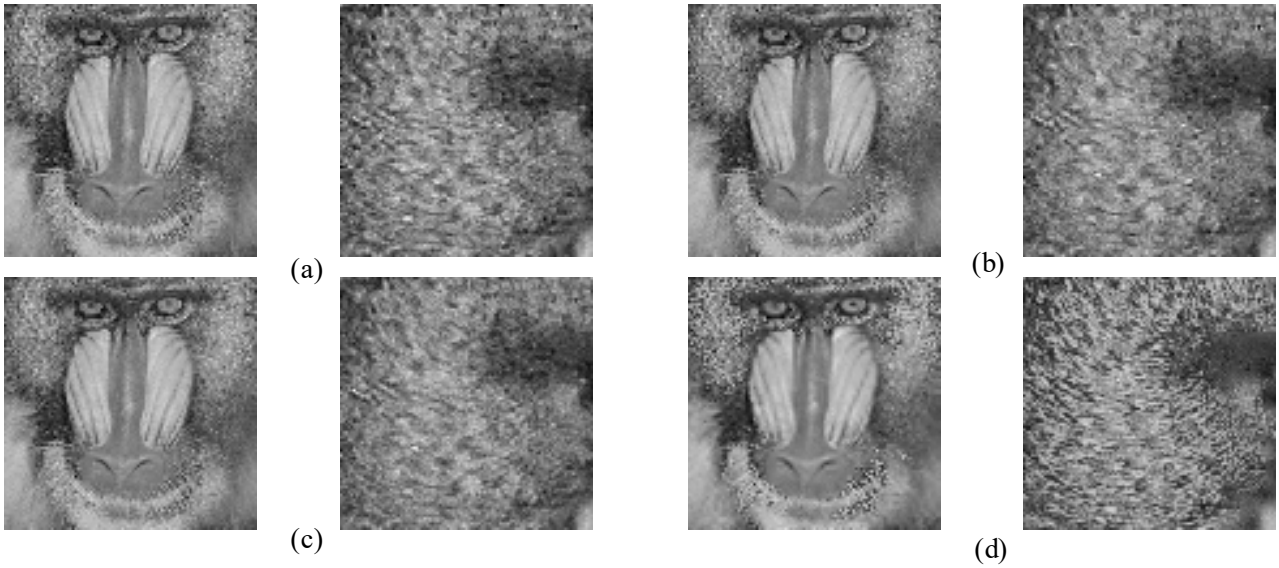

Fig. 3. Reconstructions of the Mandrill image at a sub-sampling rate of 0.3 (a)BCS-SPL-DCT (b)BCS-SPL-DWT (c)BCS-SPL-DDWT (d)Proposed algorithm

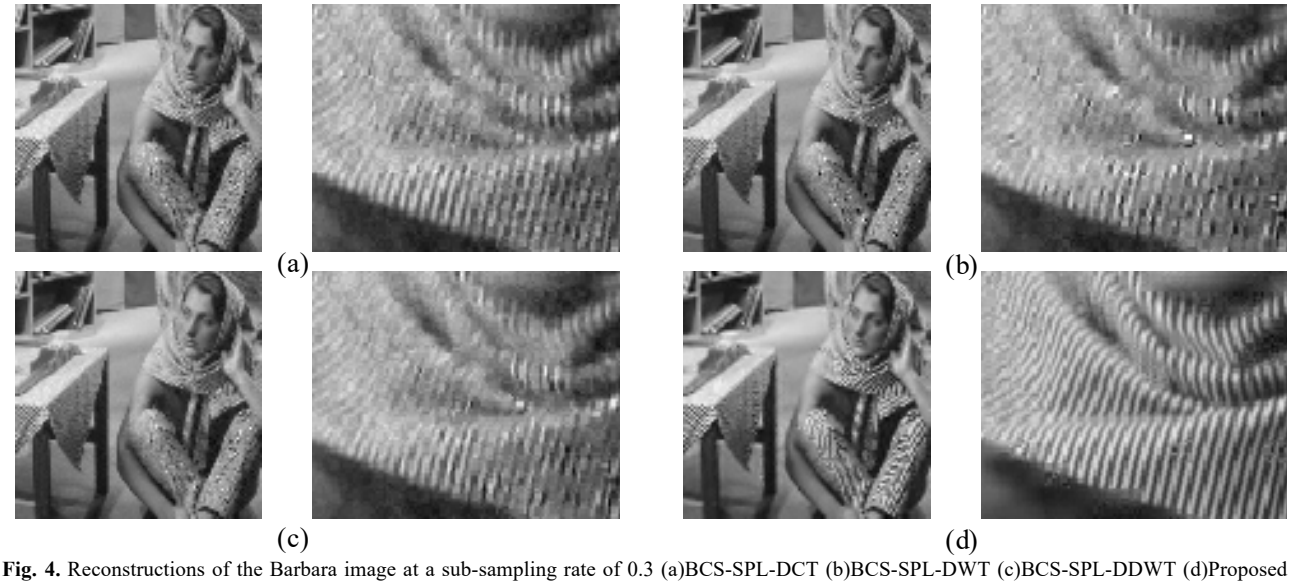

Fig. 4. Reconstructions of the Barbara image at a sub-sampling rate of 0.3 (a)BCS-SPL-DCT (b)BCS-SPL-DWT (c)BCS-SPL-DDWT (d)Proposed algorithm

Fig. 5. Reconstructions of the Cameraman image at a sub-sampling rate of 0.3 (a)BCS-SPL-DCT (b)BCS-SPL-DWT (c)BCS-SPL-DDWT (d)Proposed algorithm

5. Conclusion

A mathematical model was developed to reconstruct the texture details of the images accurately. The texture features of the images were extracted by the three-level wavelet transform, and the texture complexity was analyzed by the gray level co-occurrence matrix. The block sizes of the images were automatically adjusted, and the sub-sampling rates were adaptively allocated due to the texture complexity. The following conclusions could be drawn:

(1) The texture details of reconstructed images are abundant, and the image edges are clear. Superior visual qualities are also achieved. The reconstruction effect of blocks with complex textures is substantially improved, and the blocking artifacts are effectively eliminated.

(2) The reconstruction qualities are improved for images with different texture complexity at different sub-sampling rates. The advantage is particularly evident with the increase in the sub-sampling rate.

(3) At the sub-sampling rate of 0.3, a 2.42–3.3 dB gain in reconstruction PSNR for Barbara image over the original BCS-SPL is achieved, and no visual differences are noted between the reconstructed and original texture blocks.

Thus, the variable block size and adaptive sub-sampling rate are adopted in the proposed algorithm to reconstruct the texture details of the images accurately. However, the threshold of texture complexity is determined by the simulation experiments. The efficient determination of the threshold should be considered in future studies.

Acknowledgements

This work was supported by Natural Science Foundation of Liaoning Province of China(Grant No. 20170540720) and Foundation of Liaoning Educational Committee(Grant No. LQ2019019).

References

1. Donoho, D. L, "Compressed sensing". *IEEE Transactions on Information Theory*, 52(4), 2006, pp.1289-1306.
2. Liu, X., Zhang, J., Li, X., Zhou, S-W., Zhou, S-Y., Kim, H.-J., "A block compressed sensing for images selective encryption in cloud". *Computers, Materials and Continua*, 61(3), 2019, pp.29-41.
3. Li, M., Xiao, D., Zhang, Y., "Reversible data hiding in block compressed sensing images". *ETRI Journal*, 38(1), 2016, pp.159-163.
4. Zhu, R., Li, G., Guo, Y., "Block-compressed- sensing-based reconstruction algorithm for ghost imaging". *OSA Continuum*, 2(10), 2019, pp.2834-2843.
5. Bora, D. R., Jangale, S., "Block compressed sensing of videos: A case study". *IOSR Journal of Computer Engineering*, 20(3), 2018, pp.49-53.
6. Tsaig, Y., Donoho, D. L., "Extensions of compressed sensing". *Signal Processing*, 86(3), 2006, pp.549-571.
7. Mun, S., Fowler, J. E., "Block compressed sensing of images using directional transforms". In: *Proceedings of the 16th International Conference on Image Processing,* Cairo, Egypt: IEEE, 2009, pp.3021-3024.
8. Spurthi, S., Chakraborty, P., "Block based compressed sensing algorithm for medical image compression". *International Journal of Engineering and Computer Science*, 5(5), 2016, pp.16704-16707.
9. Haltmeier, M., Berer, T., Moon, S., Burgholzer, P., "Compressed sensing and sparsity in photoacoustic tomography". *Journal of Optics*, 18(11), 2016, pp.114004.
10. Unde, A. S., P.P., D., "Block compressive sensing: Individual and joint reconstruction of correlated images". *Journal of Visual Communication and Image Representation*, 44, 2017, pp.187-197.
11. Cao, Y., Gong, W., Zhang, B., Zeng, F., Bai, S., "Optimal permutation based block compressed sensing for image compression applications". *IEICE Transactions on Information and Systems*, E101-D(1), 2018, pp.215-224.
12. Eslahi, N., Aghagolzadeh, A., Andargoli, S. M. H., "Image/video compressive sensing recovery using joint adaptive sparsity measure". *Neurocomputing*, 200, 2016, pp.88-109.
13. Bigot, J., Boyer, C., Weiss, P., "An analysis of blocks sampling strategies in compressed sensing". *IEEE Transactions on Information Theory*, 62(4), 2016, pp.2125-2139.
14. George, S. N., Pattathil, D. P., "A secure LFSR based random measurement matrix for compressive sensing". *Sensing and Imaging*, 15(1), 2014, pp.85.

15. Fowler, J. E., Mun, S., Tramel, E. W., "Multiscale block compressed sensing with smoothed projected landweber reconstruction". In: *Proceedings of the 19th European Signal Processing Conference*, Barcelona, Spain: IEEE, 2011, pp.564-568.
16. Li, Y., Zhao, R., Zhang, F., "Adaptive multi-scale block compressed sensing algorithm based on edge and direction estimation". *Journal of Signal Processing*, 31(4), 2015, pp.407-413.
17. Cheng, D., Gao, L., Chen, L., Chen, G., Tu, Y., "Adaptive multiscale block compressed sensing algorithm". *Journal of Image and Graphics*, 22(9), 2017, pp.1175-1182.
18. Cheng, D., Shao, L., Li, Y., Guan, Z., "Multi-scale block adaptive sampling rate compression sensing algorithm". *Laser & Optoelectronics Progress*, 56(3), 2019, pp.031005.
19. Li, R., Duan, X., Guo, X., He, W., Lv, Y., "Adaptive compressive sensing of images using spatial entropy". *Computational Intelligence and Neuroscience*, 2017, pp.9059204.
20. Wang, Y., Zhou, C., Xiong, C., Shu, Z., "Enhanced block compressed sensing of images based on total variation using texture information". *Computer Science*, 43(2), 2016, pp.307-310, 315.
21. Cai, X., Xie, Z., Huang, H., "An adaptive reconstruction algorithm for image block compressed sensing under low sampling rate". *Journal of Chinese Computer Systems*, 37(3), 2016, pp.612-616.